16th World Conference on Earthquake Engineering, 16WCEE 2017

Santiago Chile, January 9th to 13th 2017

Paper N° 3696

Registration Code: S-G1463753700

ESTIMATION OF SUBSURFACE S-WAVE VELOCITY STRUCTURE IN YANGON CITY, MYANMAR USING MICROTREMORS

Y. Hirokawa[1], S. Matsushima[2], H. Kawase[3], Myo Thant[4], Tun Naing[5]

[1] *Former Graduate Student, Toyo Engineering, yuki.hirokawa@zeisei.dpri.kyoto-u.ac.jp*
[2] *Professor, Disaster Prevention Research Institute, Kyoto University, matsushima@sds.dpri.kyoto-u.ac.jp*
[3] *Professor, Disaster Prevention Research Institute, Kyoto University, kawase@zeisei.dpri.kyoto-u.ac.jp*
[4] *Associate Professor, Department of Geology, University of Mandalay, myothant05@gmail.com*
[5] *Associate Professor, Department of Geology, Dawei University, tunnaing1972@gmail.com*

Abstract

This study focuses on S-wave velocity structures in Yangon City, Myanmar, where the construction works have been performed without thorough consideration of present threat from strong shaking from large earthquakes. Especially, the most active and dangerous fault called the Sagaing fault is expected to cause large magnitude crustal earthquakes in the near future along the segment nearby Yangon City. Understanding the subsurface velocity structure is an important factor in mitigating seismic damages, because they can be used to estimate site amplification factors and simulate the expected strong ground motions due to crustal earthquakes nearby. In this study we investigated subsurface velocity structures based on Horizontal-to-Vertical spectral ratios (HVRs) of microtremors as well as phase velocity estimates from the vertical component array observation inside Yangon City. Several array measurements with different radius were conducted at the site. From previous studies, the observed HVRs show consistent peaks as fundamental peak at lower frequencies ranging from 0.7 to 1.3 Hz, while another peak at higher frequencies range from 20 to 40 Hz, so we focus on frequencies below few Hz to consider the velocity structure that affects the fundamental peak. An S-wave velocity structure at the array measurement site was obtained so as to make both theoretical Rayleigh wave phase velocity dispersion curves and theoretical HVRs derived from diffuse field assumption, simultaneously agree with the observed ones. As a result, we found that in order to fit the Rayleigh wave dispersion curve obtained from the smaller and larger array measurement, we need a nine-layer model with the deepest layer at 1200 m depth with Vs=1800 m/s. A layer with Vs=800 m/s exists at around 100 m below the surface as the presumable engineering bedrock, while the uppermost softest layer with Vs=140 m/s have the thickness of 1.5 m in the area.

Keywords: Myanmar; Yangon; subsurface structure; microtremor; dispersion curve; diffuse field

1. Introduction

The Republic of the Union of Myanmar (Myanmar) is a Southeast Asian country located in an earthquake-prone area on the boundary between the Indian plate and the Eurasian plate (Fig. 1). As a consequence of accumulated tectonic stress in this structurally complex region, many geological faults are formed in Myanmar. Among these faults, the Sagaing fault is a highly active right-lateral fault that runs through central Myanmar from north to south. A number of large earthquakes have occurred in Myanmar along the Sagaing fault in the past (Fig 2). The city of Yangon is located approximately 30 km west of the Sagaing fault. It is Myanmar's largest city, with a population of approximately 5 million people. Furukawa and Maung Maung [1] performed analysis to re-determine the epicenters of historical earthquakes that have occurred since 1918 in the area around the Sagaing fault. According to their analysis, earthquakes have not occurred following the three successive large earthquakes that occurred between 1929 and 1930 roughly in the same area. Pailoplee and Choowong [2] analyzed the potential of future earthquakes occurring in Southeast Asia in an area centered on Myanmar. This study suggests that the next M_w 7.2 to 7.5 earthquake may occur in the Sagaing fault region within the next two decades. It also suggests the possibility of an M_w 8.0 earthquake occurring in the area.

As these previous surveys demonstrate, Yangon is located in a very seismically active area along the Sagaing fault. In case of an earthquake, serious damage may occur to the city. After the democratization of Myanmar, new construction took place without thorough consideration of earthquakes. In order to estimate the possible strong shaking for future earthquakes it is necessary to know the subsurface structure in detail. Boring explorations have been conducted for the purpose of constructions to a depth of approximately 50 m, but they are not open to the public so the information of the subsurface structure is limited. Therefore, in this study we attempt to estimate the subsurface structure from microtremor measurements, which is much easier than cost effective than observing earthquake ground motions. It is nondestructive and no vibrations or noise will be observed like other measurements of exploration methods with active sources, such as reflection and refraction surveys. There are two methods for the technique to measure microtremors: array observation and single-station observation. This study conducts surveys by using both array and single-station observation methods in Yangon.

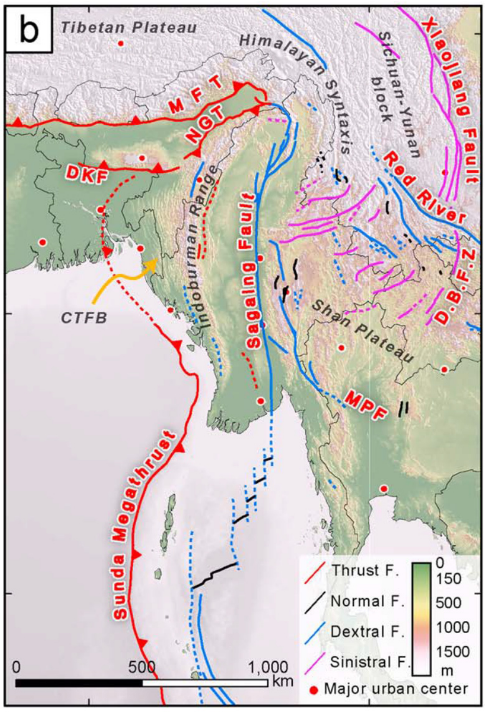

Fig. 1 –Map of tectonic situation around Yangon including plate boundaries and major faults [3]. Sunda plate and South China plate constitute of parts of Eurasian plate.

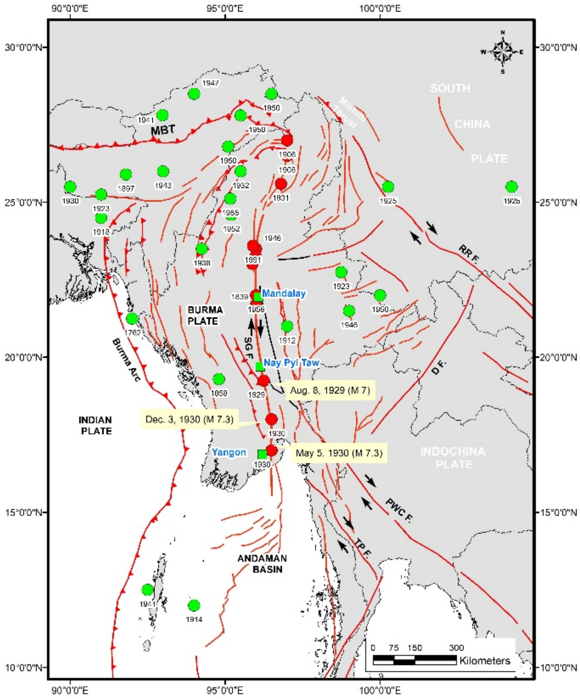

Fig. 2 – Epicenters of past earthquakes in Myanmar developed from ISC earthquake catalog [4] and previous studies [5-6]. The red circles denote the epicenter of earthquakes estimated to have occured on the Sagaing Fault.

Hirokawa et al. [7] made single-station microtremor observations in a wide area of the city of Yangon to estimate the subsurface structure. In the process of the analysis for the observed data, horizontal-to-vertical spectral ratios (HVRs) of microtremors were calculated. The observed HVRs are compared to theoretical HVRs, which are calculated based on the new theory assuming a diffuse wave field [8]. This new theory enables us to calculate HVRs not only for horizontal (flat-layered) subsurface structure but also for sites with lateral heterogeneity [9]. Also, the new theory makes it possible to evaluate not only peak frequencies but amplification of HVRs unlike conventional methods. The new theory was tested for observed HVRs in several locations [10-12]. In their study, the velocity profile was constrained only for the layers above the assumed engineering bedrock with Vs=800 m/s, so a task remained to determine the deeper structure.

2. Microtremor Observations and Analysis

We used two systems for microtremor observations. One was the combination of SMAR-6A3P (manufactured by Akashi Corporation (now Mitutoyo, Ltd.), a portable three-component acceleration seismograph with a 0.1–10,000 times amplifier and DATAMARK LS8800 (manufactured by Hakusan Kogyo Co., Ltd.), a data logger, which was used for small array observation. Other was the combination of VSE-11&VSE-12 (manufactured by Tokyo Sokushin Co., Ltd.), a servo velocity-meter, LS8800 and the amplifier of SMAR-6A3P, which was used for large array observation. The sampling frequency for small array observation and large array observation was 200 Hz and 100 Hz, respectively. The amplifier was set to 500 times or 50 times for small or large array observation, respectively. A 50-Hz low-pass filter was used and the Global Positioning System (GPS) was used for time calibration.

In this study, we use microtremor data from array measurements in order to obtain the phase velocity dispersion curves of Rayleigh waves as well as HVRs to constraint the subsurface structure from surface to layers deeper than the engineering bedrock. Fig. 3a shows the map of the city of Yangon showing location of the observation site and the observation points of the large array. The large array consists of two radius, 200 m and 500 m, which is indicated by yellow circles in Fig. 3b. The small array consists of 3 m, 10 m, 30 m, and 90 m, which the 90 m radius circle is indicated in light green circles in Fig. 3b. Tables 1 and 2 shows the location of the observation points for the large array and small array, respectively.

(a) Location of the observation site

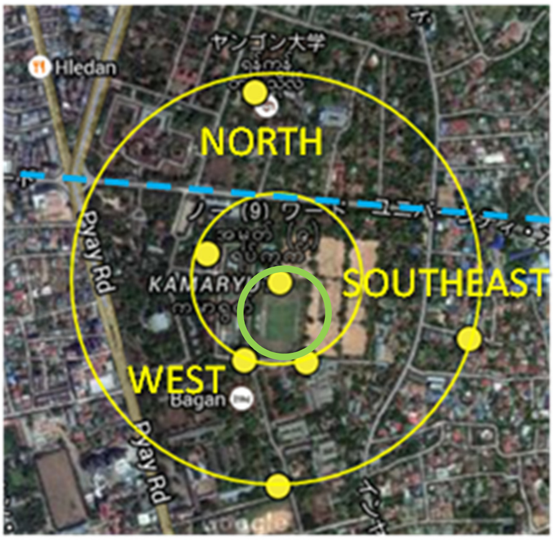

(b) Observation points of the large arrays

Fig. 3 – Map of the city of Yangon showing (a) the location of the observation site and (b) the observation points for the large array. The blue and red circles in (a) shows the large and small arrays, respectively. The yellow color-filled circles in (b) denote the observation points of the large arrays with radius of 200m and 500m. The light green circle in (b) denotes the location of the small array.

2.1 Analysis of Single-Station Data

For the single-station analysis, the observation records were divided into 40.96-second segments with an overlap of 50% of the duration. The effect of large input noise, such as traffic, human activity, etc. was minimized by extracting the segment with noise comparing between the root mean square of all segments and of each segment for the three components. Prior to the analysis, the waveforms were baseline corrected for each segment. To reduce the influence from the end of the segments, a cosine taper was used for 0.5% duration in the beginning and end of each segment. For each segment, the power spectrums S_{NS}, S_{EW}, and S_{UD} were calculated and smoothed by Parzen window with a width of 0.1 Hz. The HVRs were calculated using S_{NS}, S_{EW}, and S_{UD} as shown in Eq. (1).

$$\mathrm{HVRs} = \sqrt{\frac{S_{NS} + S_{EW}}{S_{UD}}} \tag{1}$$

Table 1 – The conditions of the observation points for the large array

Date	**Array radius [m]**	**Start**	**End**	**Duration [min.]**	**Position**	**Lat. [deg.]**	**Lon. [deg.]**	**Sampling Freq. [Hz]**
2015/8/8	200	16:38	17:04	26	center	16.82403	96.13583	200
					southeast	16.82235	96.13494	200
					north	16.82484	96.13402	100
					west	16.82233	96.13642	200
	500	17:42	18:10	28	center	16.81944	96.13583	200
					southeast	16.81944	96.13575	200
					north	16.82856	96.13516	100
					west	16.82285	96.14037	200

Table 2 – The conditions of the observation points for the small array (after [5])

Date	Array radius [m]	Start	End	Duration [min.]	Center Position		Position	x-coordinate [m]	y-coordinate [m]	Sampling Freq. [Hz]
					Lat. [deg.]	Lon. [deg.]				
2013/11/23	90	10:08	10:31	23	16.82333	96.13528	center	0.0	0.0	200
							north	-33.7	79.7	200
							south	-44.4	77.9	200
							east	90.5	-26.7	200
	30	10:45	11:20	35	16.82333	96.13528	center	0.0	0.0	200
							north	-15.0	26.0	200
							south	-15.0	-25.1	200
							east	30.0	0.0	200
	10	11:24	11:40	16	16.82333	96.13528	center	0.0	0.0	200
							north	-5.0	8.7	200
							south	-5.0	-8.4	200
							east	10.0	0.0	200
	3	11:44	12:01	17	16.82333	96.13528	center	0.0	0.0	200
							north	-1.5	2.6	200
							south	-1.5	-2.5	200
							east	3.0	0.0	200

Fig. 4 shows the HVRs of the observed microtremor at the center positions for 200 m large array and small array, as a sample of the observed HVRs at the observation site. There is a small amplitude peak around 0.8 Hz and a sharp peak at high frequencies. These characteristics are common among the observed HVRs.

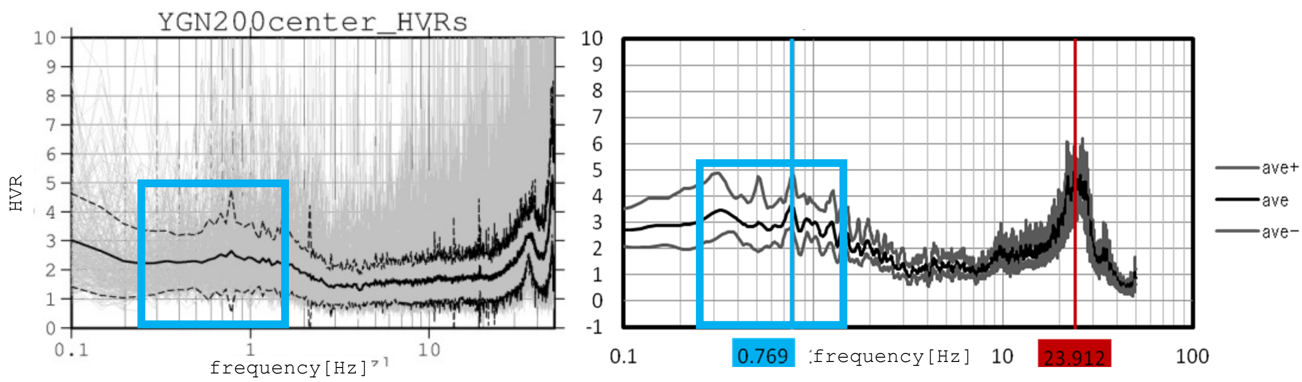

(a) HVR of velocity-meter

(b) HVR of accelerometer

Fig. 4 – HVRs at the center position of (a) large array by velocity-meter and (b) small array by accelerometer.

2.2 Analysis of Array Data

Analysis of array measurement data first involves phase-velocity analysis, i.e. determining the dispersion curve of Rayleigh wave phase velocity from the observed data by using an array analysis program BIDO [13]. Same treatments are performed as single-station observations prior to the analysis. For the analysis, the noise-compensated CCA (nc-CCA method) [14] and conventional SPAC method [15] was applied in this study. The nc-

CCA method is a revised method of CCA method [16] as to lower the effect of unsteady noise and prevents phase velocity from being underestimated. Both methods are the extended SPAC methods available for center less array measurement and applicable in a wide wavelength range especially in low frequency ranges. The parameters used for obtaining the dispersion curve of phase velocity of Rayleigh waves for the large array is shown in Table 3.

Fig. 5 shows the dispersion curve of the phase velocity of Rayleigh waves obtained from the small and large arrays using nc-CCA and SPAC methods. In Fig. 5a, the blue, green, purple and red open circles denote the phase velocity obtained from the smaller arrays with radius of 89 m, 30 m, 10 m, and 3 m, respectively. The orange filled circle is the representative phase velocity for the small array. The blue and green open circles in Fig. 5b denotes the phase velocity obtained from the 200 m and 500 m large arrays, respectively. The red and orange filled circles in Fig. 5b denotes the representative phase velocity for the large and small arrays, respectively. The color filled circles will be used for inversion of the subsurface velocity structure.

Table 3 – The parameters used for obtaining the dispersion curve of phase velocity of Rayleigh waves for large array

Array radius [m]	High Pass Filter [Hz]	Low Pass Filter [Hz]	No. of Segments	Parzen Window Width [Hz]
200	0.5 (0.452)	2.0 (2.4)	35	0.1
500	0.1 (0.092)	1.0 (1.2)	39	0.1

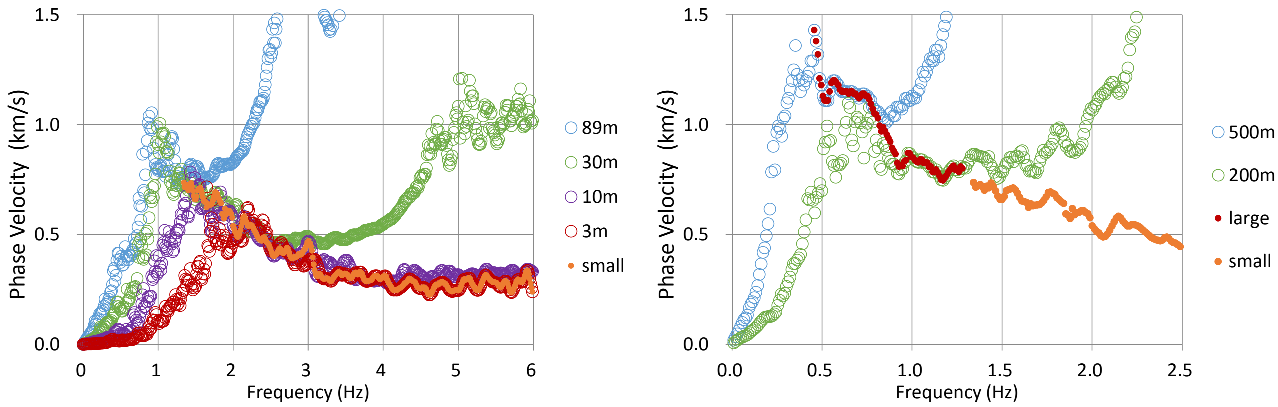

(a) Small array (after [5]) (b) Large array

Fig. 5 – Dispersion curve of Rayleigh waves phase velocity obtained from (a) small array and (b) large array. The phase velocity for small array (orange filled circle) is constrained by arrays with radius of 3 m and 10 m. The phase velocity for large array (red filled circle) is constrained by the 200 m and 500 m arrays.

3. Estimation of the Subsurface Velocity Structure

In order to estimate the subsurface velocity structure, we used both dispersion curve of Rayleigh wave phase velocity and HVRs obtained from microtremor observation in Chapter 2.

To construct the initial model for conducting the estimation, the top three layers were modeled by referring to the results of boring exploration performed near the observation site by Suntec Engineerings Co. Ltd, reaching the depth of 50 m [7]. The S-wave velocity were converted from N values of the boring exploration by using Imai's equations (Eqs. (2) and (3)) [17]. The deeper layers were constructed by referring to Ballard's method [18] (Eq. (4)). The method was proposed for constructing an initial model for S-wave velocity profile in an area where only limited exploration data are available. This method allows to directly estimate the S-wave velocity profile from a dispersion curve of Rayleigh wave phase velocity.

$$\mathrm{Vs(m/s)} = 80.6\mathrm{N}^{0.331} \quad \text{(Cohesionless soil)} \tag{2}$$

$$\mathrm{Vs(m/s)} = 102\mathrm{N}^{0.292} \quad \text{(Cohesive soil)} \tag{3}$$

$$\mathrm{Z} = \frac{1}{3}\lambda, \mathrm{Vsz} = 1.1\mathrm{C}_{\lambda} \tag{4}$$

By trial and error, Hirokawa et al. [7] found the least number of layers necessary to express the estimated dispersion curve obtained from the small array to be 6, one top layer, two layers in the shallow depth, two layers in the deep part, and one bottom layer. The estimated velocity profile is the hatched layers in Table 3. The P wave velocity and density of each layer is obtained from the relation between S wave velocity and P wave velocity and P wave velocity and density, shown in Eqs. (5) and (6) [19].

$$\mathrm{Vp(km/s)} = 0.9409 + 2.0947\mathrm{Vs} - 0.8206\mathrm{Vs}^{2} + 0.2683\mathrm{Vs}^{3} - 0.0251\mathrm{Vs}^{4} \tag{5}$$

$$\rho(\mathrm{g/cm^3}) = 1.6612\mathrm{Vp} - 0.4721\mathrm{Vp}^2 + 0.0671\mathrm{Vp}^3 - 0.0043\mathrm{Vp}^4 + 0.000106\mathrm{Vp}^5 \tag{6}$$

The thickness and S wave velocity of layers 6 to 8 in Table 3 was estimated by trial and error, by fitting the observed dispersion curve of Rayleigh wave phase velocity by the theoretical one. The theoretical dispersion curve is calculated by using code developed by Hisada [20]. The comparison between the best fit theoretical Rayleigh wave phase velocity calculated by the profile of Table 3 and the observed phase velocity is shown in Fig. 6a. The theoretical HVR of microtremors calculated considering the diffuse field assumption [8] is shown in Fig. 6b, compared with the observed HVR. Both observed Rayleigh wave phase velocity and HVR of microtremor is well reproduced by the theoretical ones, so the estimated velocity profile in Table 3 can be considered as the velocity profile in central Yangon.

Table 3 – The velocity profile obtained from fitting the observed dispersion curve Rayleigh wave phase velocity and H/V spectral ratio of microtremors

Layer	**Thickness [m]**	**Depth [m]**	**Vp [m/s]**	**Vs [m/s]**	**ρ [g/cm^3]**
1	1.3	1.3	1219	140	1.44
2	23.7	25	1417	250	1.58
3	25	50	1552	330	1.67
4	80	130	1844	520	1.83
5	180	310	2219	800	2.00
6	190	500	2458	1000	2.08
7	300	800	2740	1250	2.16
8	400	1200	3015	1500	2.23
9	∞	∞	3354	1800	2.29

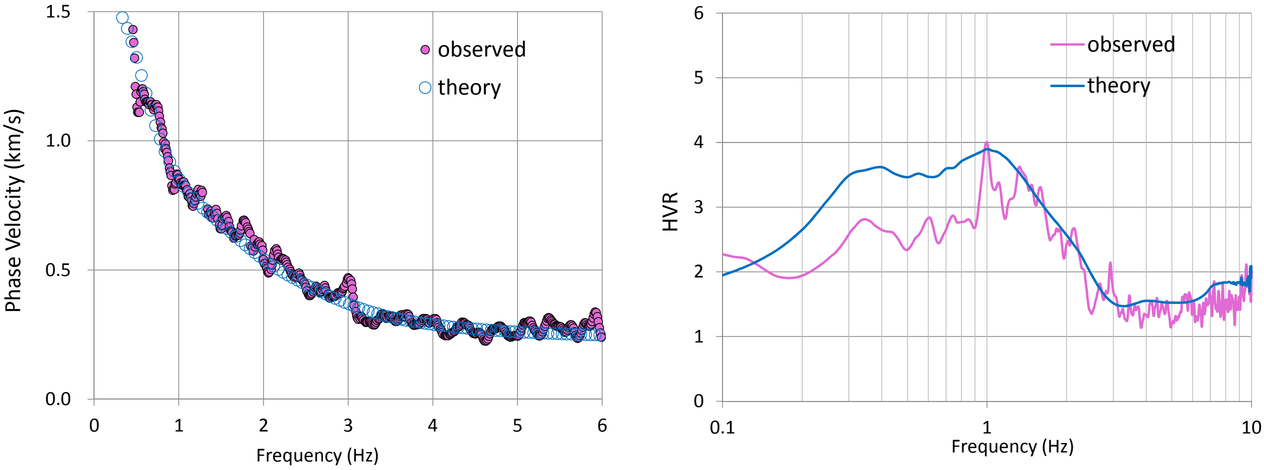

(a) Rayleigh wave phase velocity (b) HVR

Fig. 6 – Comparison of observed and theory for (a) dispersion curve of Rayleigh wave phase velocity and (b) HVR of microtoremors

4. Conclusions

We performed microtremor array observations at the athletic field of University of Yangon in the central part of the city of Yangon, Myanmar in order to investigate the subsurface velocity structures based on dispersion curve of Rayleigh wave phase velocity as well as HVRs of microtremors. Several array measurements with different radius were conducted at the site. From previous studies, the observed HVRs show consistent peaks as fundamental peak at lower frequencies ranging from 0.7 to 1.3 Hz, while another peak at higher frequencies range from 20 to 40 Hz, so we focus on frequencies below few Hz to consider the velocity structure that affects the fundamental peak. An S-wave velocity structure at the array measurement site was obtained so as to make both theoretical Rayleigh wave phase velocity dispersion curves and theoretical HVRs derived from diffuse field assumption, simultaneously agree with the observed ones.

As a result, we found that in order to fit the dispersion curve of Rayleigh wave phase velocity obtained from the smaller and larger array measurement, we need a nine-layer model with the deepest layer at 1200 m depth with Vs=1800 m/s. A layer with Vs=800 m/s exists at around 100 m below the surface as the presumable engineering bedrock, while the uppermost softest layer with Vs=140 m/s have the thickness of 1.5 m in the area.

Previously we have performed single-station observations at 27 points throughout the central urban area of Yangon. The results revealed that the primary and secondary peak frequencies in Yangon were 0.7−1.2 and 20−35 Hz, respectively. We will use the velocity structure obtained in this study to modify the velocity structure we have obtained from the HVRs of single-station observations points. These information will be used to construct a three dimensional subsurface velocity structure model to cover whole the city. For this purpose, we are also conducting strong motion observations in order to get information about the layers deeper than the layer with Vs=1800 m/s, and possibly go down to the seismic bedrock. Our ultimate goal is to use the ground structure models to predict strong ground motions in relation to earthquakes associated with the Sagaing fault, and to create seismic hazard maps as well as design input ground motions for the city of Yangon.

Acknowledgements

The authors thank the participants from Kyoto University, Yangon University and other institutes for the cooperation during the microtremor measurements. Parts of this study were supported by CRC Project of JICA AUN/SEED-net (PI Tun Naing), Supporting Program for Interaction-based Initiative Team Studies (SPIRITS) (PI Hiroshi Kawase), and Proposal type research of the "Cooperative Research by Liaison between Hub Institutes" project within the framework of "Promotion of Observation and Research Plan of Earthquakes and Volcanos for Contributing to Mitigation of Disasters" (PI Hiroshi Kawase).

References

[1] Hurukawa N and Maung Maung P (2011): Two seismic gaps on the Sagaing Fault, Myanmar, derived from relocation of historical earthquakes since 1918, *Geophysical Research Letters*, 38, L01310, doi: 10.1029/2010GL046099.

[2] Pailoplee S and Choowong M (2012): Probabilities of earthquake occurrences in Mainland, Southeast Asia, Arabian Journal of Geosciences, 6, 4993-5006, DOI 10.1007/s12517-012-0749-5.

[3] Wang Y, Sieh K, Tun ST, Lai KY, Myint T (2014): Active tectonics and earthquake potential of the Myanmar region, *Journal of Geophysical Research Solid Earth*, 119, 3767–3822, doi:10.1002/2013JB010762.

[4] International Seismological Centre (2013): *On-line Bulletin*, http://www.isc.ac.uk, International Seismological Center, Thatcham, United Kingdom.

[5] Gorshkov GP (1959): Problems of Seismotectonics and Seismicity - Zoning of the Territory of the Union of Burma. (Mineographed Manuscript).

[6] Gutenberg B, Richter CF (1954): Seismicity of the Earth and Associated Phenomena 2nd Edition, Princeton, Princeton U.P.

[7] Hirokawa Y, Matsushima S, Kawase H, Tun Naing, Myo Thant (2016): Estimation of underground structures in Yangon City, Myanmar using single-station and array measurements, *Journal of Japan Association for Earthquake Engineering*, 16 (1) Special issue: The 14th Japan Earthquake Engineering Symposium (2) 49-58, http://doi.org/10.5610/jaee.16.1_49 (in Japanese with English abstract).

[8] Sánchez-Sesma FJ, Rodríguez M, Iturrarán-Viveros U, Luzón F, Campillo M, Margerin L, García-Jerez A, Suarez M, Santoyo MA, Rodríguez-Castellanos A (2011): A theory for microtremor H/V spectral ratio: application for a layered medium, *Geophysical Journal International Express Letters* 186 (1) 221-225 doi: 10.1111/j.1365-246X.2011.05064.x.

[9] Matsushima S, Hirokawa T, De Martin F, Kawase H, Sánchez-Sesma FJ (2014): The Effect of Lateral Heterogeneity on Horizontal-to-Vertical Spectral Ratio of Microtremors Inferred from Observation and Synthetics, *Bulletin of the Seismological Society of America*, 104 (1), 381-393, doi:10.1785/0120120321.

[10] Matsushima S, Sánchez-Sesma FJ, Nagashima F, Kawase H (2011): Verification of the Velocity Structure in Mexico Basin Using the H/V Spectral Ratio of Microtremors, AGU 2011 Fall Meeting, S23A-2216.

[11] Tobita K, Kawase H, Matsushima S (2014): Estimation of Subsurface Structures Using Microtremors in the Southern Part of the Osaka Plain, *Journal of Japan Association for Earthquake Engineering*, 14 (2), 104-123, http://doi.org/10.5610/jaee.14.2_104 (in Japanese with English abstract).

[12] Fukihara K, Matsushima S, Kawase H (2015): Identification of the velocity structure model of Kyoto basin for strong motion prediction using observed earthquake and microtremor motions, *Journal of Japan Association for Earthquake Engineering*, 15 (6), 60-76, http://doi.org/10.5610/jaee.15.6_60 (in Japanese with English abstract).

[13] Tada T, Cho I, Shinozaki Y (2010): Analysis of Love-Wave Components in Microtremors, *Proceedings of the 7th International Conference on Urban Earthquake Engineering*, Tokyo Institute of Technology.

[14] Tada T, Cho I, Shinozaki Y (2007): Beyond the SPAC method: Exploiting the wealth of circular-array methods for microtremor exploration, *Bulletin of Seismological Society of America*, 97(6), 2080−2095.

[15] Okada H (2003): The microtremor survey method, *Society of Exploration Geophysics of Japan*, Translated by Koya Suto, Geophysical Monograph Series, Volume 12.

[16] Cho I, Tada T, Shinozaki Y (2004): A new method to determine phase velocities of Rayleigh waves from microseisms, *Geophysics*, 69, 1535−1551.

[17] Imai T (1977): P and S wave velocities of the ground in Japan, *Proceeding of IX International Conference on Soil Mechanics and Foundation Engineering*, (2), 257−260.

[18] Ballard RF Jr. (1964): Determination of ground shear moduli at depth by in situ vibratory techniques, *U.S. Army Engineer Waterways Experiment Station*, Vicksburg, Miss., Misc. Paper No. 4, 691.

[19] Ludwig WJ, Nafe JE, Drake CL (1970): Seismic Refraction, the Sea 4, Edited by A. Maxwell, Wiley Inter Science, New York, 53−84.

[20] Hisada Y (1997): Efficient methods for computing Green's functions and normal mode solutions for layered half-spaces, *Journal of Structural and Construction Engineering*, Architectural Institute of Japan, No. 501, 49−56.